

Easy-Poly: A Easy Polyhedral Framework For 3D Multi-Object Tracking

Peng Zhang

52205901027@stu.ecnu.edu.cn
East China Normal University
Shanghai, China

Xin Lin*

xlin@cs.ecnu.edu.cn
East China Normal University
Shanghai, China

Xin Li

51194506020@stu.ecnu.edu.cn
Shanghai Jiao Tong University
Shanghai, China

Liang He

lhe@cs.ecnu.edu.cn
East China Normal University
Shanghai, China

ABSTRACT

Recent advancements in 3D multi-object tracking (3D MOT) have predominantly relied on tracking-by-detection pipelines. However, these approaches often neglect potential enhancements in 3D detection processes, leading to high false positives (FP), missed detections (FN), and identity switches (IDS), particularly in challenging scenarios such as crowded scenes, small-object configurations, and adverse weather conditions. Furthermore, limitations in data preprocessing, association mechanisms, motion modeling, and life-cycle management hinder overall tracking robustness. To address these issues, we present **Easy-Poly**, a real-time, filter-based 3D MOT framework for multiple object categories. Our contributions include: (1) An *Augmented Proposal Generator* utilizing multi-modal data augmentation and refined SpConv operations, significantly improving mAP and NDS on nuScenes; (2) A **Dynamic Track-Oriented (DTO)** data association algorithm that effectively manages uncertainties and occlusions through optimal assignment and multiple hypothesis handling; (3) A **Dynamic Motion Modeling (DMM)** incorporating a confidence-weighted Kalman filter and adaptive noise covariances, enhancing MOTA and AMOTA in challenging conditions; and (4) An extended life-cycle management system with adjustive thresholds to reduce ID switches and false terminations. Experimental results show that Easy-Poly outperforms state-of-the-art methods such as Poly-MOT and Fast-Poly [15], achieving notable gains in mAP (e.g., from 63.30% to 64.96% with LargeKernel3D) and AMOTA (e.g., from 73.1% to 74.5%), while also running in real-time. These findings highlight Easy-Poly's adaptability and robustness in diverse scenarios, making it a compelling choice for autonomous driving and related 3D MOT applications. The source code of this paper will be published upon acceptance.

*corresponding author

Permission to make digital or hard copies of all or part of this work for personal or classroom use is granted without fee provided that copies are not made or distributed for profit or commercial advantage and that copies bear this notice and the full citation on the first page. Copyrights for components of this work owned by others than the author(s) must be honored. Abstracting with credit is permitted. To copy otherwise, or republish, to post on servers or to redistribute to lists, requires prior specific permission and/or a fee. Request permissions from permissions@acm.org.
ICMR '25, June 30-July 3, 2025, Chicago, USA

© 2025 Copyright held by the owner/author(s). Publication rights licensed to ACM.
ACM ISBN 978-x-xxxx-xxxx-x/YY/MM... \$15.00
<https://doi.org/10.1145/nnnnnnn.nnnnnnn>

CCS CONCEPTS

• **Computing methodologies** → **Tracking**.

KEYWORDS

Computer vision; Autonomous driving; 3D object detection; 3D multi object tracking; Deep learning; Kalman filter

ACM Reference Format:

Peng Zhang, Xin Li, Xin Lin, and Liang He. 2025. Easy-Poly: A Easy Polyhedral Framework For 3D Multi-Object Tracking. In *Proceedings of Proceedings of the 2025 International Conference on Multimedia Retrieval (ICMR '25)*. ACM, New York, NY, USA, 9 pages. <https://doi.org/10.1145/nnnnnnn.nnnnnnn>

1 INTRODUCTION

Recent years have witnessed significant advancements in 3D multi-object tracking (3D MOT), largely driven by the demands of autonomous driving, robotics, and mixed reality applications. The research trend has increasingly leaned toward the fusion of multi-modal data to enhance both reliability and accuracy [7, 21].

Traditional filtering techniques have coexisted with deep learning-based approaches, each contributing to robust 3D MOT systems. Nonetheless, most existing pipelines predominantly focus on the tracking stage, devoting less attention to improving 3D object detection itself. For instance, Poly-MOT and Fast-Poly employ the FocalsConv [5] framework together with detectors such as CenterPoint [31] and LargeKernel3D [6], but they do not thoroughly explore data augmentation or convolutional optimization in multi-modal settings. Moreover, they exhibit high identity switches (IDS), false negatives (FN), and false positives (FP), reflecting suboptimal performance in crowded scenarios, small-object detection, and adverse weather. These shortcomings underscore the need for more comprehensive methods that can efficiently integrate detection improvements with advanced filtering, robust association, and effective life-cycle management.

In this work, we propose **Easy-Poly**, a real-time filter-based 3D MOT method that follows the *tracking-by-detection* (TBD) paradigm, supporting multiple object categories and offering substantial improvements in complex environments. First, we build a **Augmented Proposal Generator** based on FocalsConv. This generator substantially elevates detection quality by incorporating refined sparse

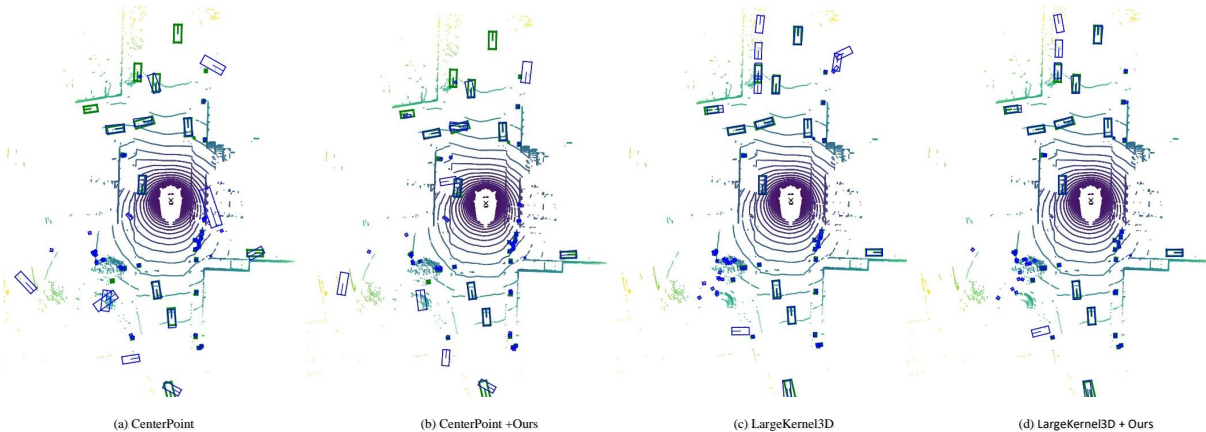


Figure 1: Data augmentation effect of CenterPoint and LargeKernel3D in multi-modal mode. It illustrates the performance gains of FocalsConv in 3D object detection. (a) and (b) present CenterPoint results, while (c) and (d) showcase LargeKernel3D outcomes. Notably, (a) and (c) utilize the baseline FocalsConv model, whereas (b) and (d) employ our augmented proposal generator, demonstrating reduced false negatives and false positives. This comparison also highlights our augmented proposal generator’s superiority over original detectors particularly in handling small objects and crowded scenes.

convolution operations and multi-modal data augmentation, leading to notable improvements in dense-traffic scenes and for small-object categories. Then, we introduce a carefully optimized *Easy-Poly* pipeline (Figure 2) that orchestrates the flow of high-quality detections through pre-processing, association, matching, estimation, and life-cycle management. Specifically, we integrate **Score Filtering (SF)** and Non-Maximum Suppression (NMS) to prune low-confidence detections, apply a **Dynamic Track-Oriented (DTO)** module to handle ambiguous data association and propose a *Dynamic Motion Modeling (DMM)* strategy that infuses confidence weighting into Kalman filter updates while adaptively adjusting both measurement and process noise covariances. These enhancements collectively mitigate false positives, reduce tracking failures, and boost the robustness of tracking.

Extensive experiments on the nuScenes dataset validate the efficacy of Easy-Poly, demonstrating superior detection and tracking performance compared to Poly-MOT and Fast-Poly baselines. With the augmented proposal generator, *CenterPoint* achieves an mAP improvement from **63.86%** to **64.89%**, while *LargeKernel3D* improves from **63.30%** to **64.96%**. Moreover, in 3D MOT, Easy-Poly raises CenterPoint’s AMOTA from **73.1%** to **74.5%**, and LargeKernel3D reaches **75.0%** AMOTA at **34.9 FPS**—almost doubling the inference speed of the baseline. Our framework thereby offers an efficient, versatile, and more reliable solution for real-world autonomous driving, underscoring the importance of synergistic improvements in both detection and tracking modules.

This paper makes the following key contributions:

- We propose a novel **Augmented Proposal Generator** that integrates refined sparse convolution and multi-modal data augmentation, significantly improving 3D detection quality in dense-traffic and small-object scenarios.
- We introduce an **Easy-Poly** pipeline encompassing pre-processing, data association, and motion modeling. Notably, we design a **DTO** algorithm for robust association under

ambiguous conditions and a **DMM** module that adaptively adjusts noise covariances.

- We incorporate **confidence-weighted Kalman filtering** and **dynamic threshold management** into life-cycle management, enhancing tracking accuracy and robustness in adverse weather and complex road conditions.
- Extensive experiments on nuScenes show that Easy-Poly outperforms Poly-MOT and Fast-Poly baselines in both detection (mAP, NDS) and MOT metrics (AMOTA, MOTA, FPS), validating the effectiveness and efficiency of our design.

2 RELATED WORK

2.1 3D Object Detection

3D object detection in autonomous driving has seen significant advancements in recent years, with methods primarily categorized based on sensor modalities: **camera-based**, **point cloud-based**, and **multi-modality-based** approaches [24]. Current research trends encompass various techniques within these categories, including monocular and multi-camera systems, Bird’s Eye View (BEV) representations, and pseudo-LIDAR technologies for camera-based methods. Point cloud-based approaches have explored voxel-based, point-voxel hybrid, BEV, 4D radar, spatiotemporal, and data augmentation techniques. Multi-modal methods focus on deep fusion and cross-modal interaction strategies.

LIDAR-only Detectors. Point-cloud processing methods in LIDAR-based systems can be broadly classified into three categories. The first category focuses on learning objective-based approaches, such as anchor-based [17] and anchor-free [8] methods. The second category emphasizes data representation-based approaches, including point-based, grid-based, point-voxel hybrid, range-based, and 4D radar methods. The third category includes auxiliary methods like data augmentation [10], spatio-temporal sequence analysis, and pseudo-labeling techniques. While LIDAR-based object detection excels in speed and accuracy, the inherent sparsity of point

clouds can lead to missed detections, particularly for small and distant objects. To address these limitations, multi-modal fusion approaches have emerged as a promising solution, leveraging the complementary strengths of camera and LIDAR modalities.

Multi Modal Fusion.

Multi-modal approaches encompass various fusion paradigms, including camera-radar, camera-LIDAR [15, 16], camera-4D radar, LIDAR-4D radar, and LIDAR-radar combinations. Camera-LIDAR fusion strategies can be categorized into three primary types: (1) early fusion, which combines raw sensor data prior to feature extraction [14, 23]; (2) deep fusion, integrating features at multiple network levels [15, 16]; and (3) late fusion, merging high-level features or detection results [19, 20]. The integration of diverse sensor modalities (e.g., image, point cloud, millimeter-wave radar, depth, and 4D radar data) has become crucial for enhancing detection accuracy. We propose a novel camera-radar feature fusion approach that synergistically leverages the complementary strengths of image and point cloud data. By incorporating advanced data augmentation techniques, our method achieves state-of-the-art accuracy and robustness in 3D object detection, particularly in challenging scenarios and adverse weather conditions.

2.2 3D Multiple Object Tracking

3D MOT is a critical component in autonomous driving perception systems, with increasing real-world applications. Despite its relatively recent emergence, the field has seen significant advances in the past decade. AB3DMOT [29] pioneered the extension of the **Tracking-by-Detection (TBD)** framework in 3D space, establishing an effective baseline. Subsequent work has focused on improving tracking accuracy by addressing challenges such as occlusion, data association, and long-term tracking in dynamic environments. The TBD framework features a well-established pipeline, dividing 3D MOT into four components: pre-processing, estimation, association, and life-cycle.

Poly-MOT and Fast-Poly are efficient 3D MOT methods based on TBD framework. Despite their status as advanced 3D MOT methods, these approaches continue to face significant challenges. These include poor tracking performance under adverse weather conditions, difficulties in handling crowded scenes and small objects, as well as errors in trajectory management. In response to these limitations, our proposed Easy-poly framework specifically addresses these issues by introducing a series of innovative solutions.

Pre-processing. While prior work [16, 22, 26] has focused primarily on tracking algorithms, the object detection component has received less attention. In contrast, Easy-Poly emphasizes multi-modal data augmentation for K3D detection and incorporates optimized Non-Maximum Suppression (NMS) threshold parameters. These enhancements significantly improve small object detection and crowded scene handling capabilities.

Estimation. This module utilizes filters (Linear Kalman Filter [12, 22, 26, 30], Extended Kalman Filter [16], Point Filter [2, 31], etc.), along with motion models, to perform two functions: (1) Predict the alive tracklets to achieve temporal alignment and association with the detection. (2) Update the matched tracklets with the corresponding observations, preparing prior information for downstream. To enhance the AMOTA score, Easy-poly optimizes

the BICYCLE model parameters through grid search or Bayesian optimization. In the motion module, we integrate object detector confidence as a weighting factor in Linear and Extended Kalman Filters, which is DMM, improving 3D object tracking accuracy and robustness.

Association. As the core of the system, this module establishes tracklet-observation similarity and resolves matching correspondence. Geometry-based (IoU [27, 29], GIoU [16, 22, 26], Euclidean [2, 12, 30], NN distance [7, 9, 25, 32], etc.) and appearance-based are the commonly used affinity metrics. Despite advancements in association techniques like Fast-Poly, addressing uncertainties and ambiguities in data association remains challenging, particularly in complex scenarios involving occlusions, missed detections, and false positives. Easy-Poly proposes to leverage DTO algorithm to solve this dilemma.

Life-cycle. This module initializes, terminates, and merges tracklets based on the count-based strategy [12, 16, 22, 26, 27, 29] or the confidence-based [2, 16, 22, 30] strategy. To mitigate issues such as premature tracking termination, we propose extending the tracking duration and dynamically adjusting the threshold. This approach enhances the robustness of our tracking framework, ensuring persistent target tracking across extended sequences.

3 METHODOLOGY

3.1 Augmented Proposal Generator

We propose an augmented proposal generator based on FocalsConv to generate more accurate 3D proposals. It involves upgrades to **CenterPoint** and **LargeKernel3D**, incorporating advanced data augmentation techniques and refined SpConv convolution methods. To tackle real-world challenges, we implement robust optimization and exception handling mechanisms for erroneous and empty frames. This leads to significant improvements in indexing efficiency during training, evaluation, and tracking phases, and substantial enhancements in object detection performance metrics, such as mAP and NDS (please see the Table 1).

Our optimized FocalsConv framework enhances the CenterPoint and LargeKernel3D methods through multi-modal data augmentation. A comprehensive analysis of augmentation techniques, including "**db_sample**", "**flip**", "**rotate**", "**rescale**", and "**translate**", reveals that a combination of **double flip** and **rotation** significantly boosts detection accuracy, especially in crowded scenes and for small object detection. The convolution process in FocalsConv is mainly implemented via the Det3D backbone network. We integrate a multi-modal LargeKernel3D module into the existing LiDAR-based LargeKernel3D framework and introduce a novel VoxelSpecific module, derived from VoxelLocal, for efficient voxelization. In the post-processing stage, FocalsConv employs rotated NMS followed by multi-class NMS. Comparative experiments with circular NMS show that PointPillars benefits the most from this approach, while LargeKernel3D achieves optimal performance with rotated NMS, and CenterPoint shows intermediate results. Table 1 presents the performance differences between the LargeKernel3D and CenterPoint methods in both the original FocalsConv model and our optimized version.

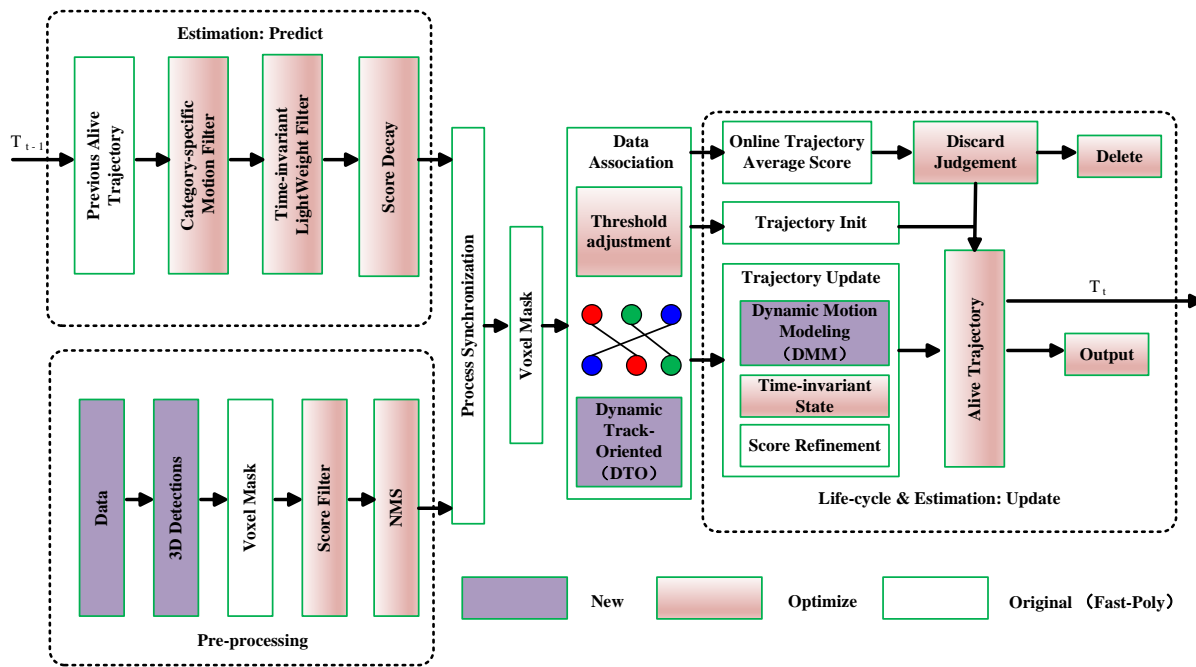


Figure 2: The pipeline of our Easy-Poly method. Real-time improvements to the baseline [15] are highlighted in distinct colors. Pink denotes the Optimization of Fast-Poly. Purple denotes the new functional modules.

Table 1: Comparison of Existing 3D object detection methods Applied to the nuScenes Val Set, except for line 2 using LIDAR only, all other methods are based on multi-modal.

Method	Detector	Augmentation	mAP	NDS
FocalsConv [5]	CenterPoint [31]	✓	63.86	69.41
FocalsConv [5]	LargeKernel3D [6]	×	63.30	69.10
Ours	CenterPoint [31]	✓	64.89	70.13
Ours	LargeKernel3D [6]	✓	64.96	70.28

3.2 Easy-Poly Framework

In this section, we introduce the details of the Easy-Poly, that processing the output from the augmented proposal generator to produce the results of 3D MOT. Easy-Poly’s pipeline is structured into five key stages: **Pre-processing**, **Association**, **Matching**, **Estimation**, and **Life-cycle**. The process unfolds as follows:

- **Pre-processing and Prediction:** For each frame, Easy-Poly employs parallel computing processes to filter 3D detections and predict existing trajectories. SF and NMS filters are applied to the detections, while specialized filters predict the motion (time-variable), score, and time-invariant states of trajectories.
- **Association and Matching:** Cost matrices are constructed for two-stage association. Voxel mask and geometry-based metric accelerate NMS and matching computations. The DTO algorithm [13] is then applied to determine matched pairs, unmatched detections, and unmatched tracklets.

- **State Update:** To optimize matrix dimensionality, time-invariant and time-variable states in matched tracklets are updated using optimized lightweight filter and Extended Kalman Filter (EKF), respectively. Scores are refined using a confidence-count mixed life-cycle approach. We propose novel DMM module, enhancing the system’s robustness to varying environmental conditions.
- **Initialization and Termination:** Unmatched detections are initialized as new active tracklets. FP agents in are identified through soft-termination, considering max-age and online average refined scores.
- **Frame Advancement:** The remaining tracklets are forwarded to downstream tasks and prepared for subsequent frame tracking.

Our Easy-Poly framework significantly enhances the previous Fast-Poly work, introducing numerous optimizations and innovations, as illustrated in Figure 2. In the pre-processing stage, we utilize the output from our augmented proposal generator, formatting the initial frame as input for the tracking module. We fine-tuned the score filter and voxel mask to enhance performance. A two-stage optimization strategy is implemented: first, we apply **Score Filtering (SF)** to eliminate low-confidence detections, effectively reducing false positives. Subsequently, **Non-Maximum Suppression (NMS)** is applied to remove highly similar bounding boxes, improving precision without significantly compromising recall. We introduce a DTO data association algorithm to address uncertainty and ambiguity in the data association phase, and implement a DMM module to enhance tracking accuracy and robustness during the life-cycle phase.

3.3 Dynamic Track-Oriented Data Association

In the data association stage, we introduce the **DTO** algorithm, a novel technique complementing traditional **Hungarian**, **Greedy**, and **Mutual Nearest Neighbor (MNN)** approaches. DTO, an optimized variant of Multiple Hypothesis Tracking (MHT), addresses object-tracking assignment uncertainties by maintaining and updating multiple association hypotheses between detections and tracks over time. This approach enables robust handling of complex scenarios as new observations become available.

The DTO data association algorithm can be summarized by the following mathematical formula in our method:

$$\mathbf{m}_{\text{det}}, \mathbf{m}_{\text{tra}}, \mathbf{u}_{\text{det}}, \mathbf{u}_{\text{tra}} = \text{DTO}(\mathbf{C}, \boldsymbol{\tau}) \quad (1)$$

$\mathbf{C} \in \mathbb{R}^{N_{\text{cls}} \times N_{\text{det}} \times N_{\text{tra}}}$ is the cost matrix between classes, detections, and tracks. If the cost matrix has a size of $N_{\text{det}} \times N_{\text{tra}}$, then $\mathbf{C} \in \mathbb{R}^{N_{\text{det}} \times N_{\text{tra}}}$, $\boldsymbol{\tau} \in \mathbb{R}^{N_{\text{cls}}}$ is the matching threshold for each class. $\mathbf{m}_{\text{det}} \in \mathbb{N}^{|\mathbf{m}_{\text{det}}|}$ is the list of matched detection indices. $\mathbf{m}_{\text{tra}} \in \mathbb{N}^{|\mathbf{m}_{\text{tra}}|}$ is the list of matched track indices. $\mathbf{u}_{\text{det}} \in \mathbb{N}^{|\mathbf{u}_{\text{det}}|}$ is the list of unmatched detection indices. $\mathbf{u}_{\text{tra}} \in \mathbb{N}^{|\mathbf{u}_{\text{tra}}|}$ is the list of unmatched track indices. Equation (1) describes the main function of the DTO algorithm, which is to take the cost matrix \mathbf{C} and the matching thresholds $\boldsymbol{\tau}$ as inputs, and output the lists of matched detection and track indices \mathbf{m}_{det} and \mathbf{m}_{tra} , as well as the lists of unmatched detection and track indices \mathbf{u}_{det} and \mathbf{u}_{tra} .

Specifically, the DTO algorithm first solves the optimal matching between detections and tracks for each class $c \in [1, N_{\text{cls}}]$ using the Hungarian algorithm on the cost matrix $\mathbf{C}[c, :, :]$, and then filters out the matches that do not satisfy the threshold τ_c . Finally, it combines the matching results from all classes to obtain the final lists of matched and unmatched detections and tracks. In summary, Equation (1) describes the inputs, outputs, and internal processing of the DTO algorithm, which is the mathematical expression of this algorithm.

The key advantage of the DTO algorithm is its ability to handle uncertainty and ambiguity in the data association problem. By maintaining multiple hypotheses, the algorithm can explore different possible associations and delay the decision-making process until more information becomes available. This can lead to more robust and accurate tracking performance, especially in challenging scenarios with occlusions, missed detections, or false alarms.

3.4 Dynamic Motion Modeling

3.4.1 Confidence Weighted Kalman Filter. In our motion model, we introduce the confidence score from the object detector as a weighting factor in the update steps of both Linear Kalman Filter and Extended Kalman Filter. This approach assigns higher weights to detections with greater confidence during state and covariance matrix updates. Consequently, this enhancement improves the accuracy (MOTA and AMOTA) and robustness of 3D object tracking. The modified update equation for the state estimate can be expressed as:

$$\hat{x}_k = \hat{x}_k|k-1 + w_k K_k (z_k - H_k \hat{x}_k|k-1) \quad (2)$$

where w_k is the confidence score of the detection at time step k , and K_k is the Kalman gain.

Similarly, the covariance update is adjusted to:

$$P_k = (I - w_k K_k H_k) P_k|k-1 (I - w_k K_k H_k)^T + w_k^2 K_k R_k K_k^T \quad (3)$$

This weighted approach effectively incorporates the reliability of detections into the filtering process, leading to more accurate and robust 3D object tracking performance.

3.4.2 Adaptive Noise Covariances. We use **Kalman Filter** for the motion model, we have introduced new dynamic adjustments to the noise covariance, including dynamic adjustment of measurement noise covariance and dynamic adjustment of process noise covariance. These are applied to both **Linear Kalman Filter** and **Extend Kalman Filter**. The dynamic adjustment of measurement noise covariance is based on the magnitude of the measurement residual to dynamically adjust the measurement noise covariance R . When the measurement residual is small, the value of R is reduced; when the measurement residual is large, the value of R is increased. The specific formula is as follows:

$$R_{\text{new}} = \begin{cases} 0.9 \cdot R, & \text{if } \|res\| < 1.0 \\ 1.1 \cdot R, & \text{if } \|res\| > 5.0 \\ R, & \text{otherwise} \end{cases} \quad (4)$$

R_{new} is the adjusted measurement noise covariance, R is the original measurement noise covariance, $\|res\|$ represents the Euclidean norm (L2 norm) of the measurement residual, $\|res\| = \sqrt{\sum_{i=1}^n res_i^2}$, where res_i is the i -th component of the residual vector. This formula expresses the following logic: If the norm of the residual is less than 1.0, R is reduced by 10%. If the norm of the residual is greater than 5.0, R is increased by 10%. If the norm of the residual is between 1.0 and 5.0, R remains unchanged. This dynamic adjustment strategy aims to adjust the behavior of the Kalman filter based on the reliability of the measurements. When the measurement residual is small, it increases the trust in the measurement (decreases R); when the measurement residual is large, it decreases the trust in the measurement (increases R).

The dynamic adjustment of process noise covariance is based on the current state to dynamically adjust the process noise covariance Q . For example, adjusting the value of Q based on the magnitude of velocity. Its formula is as follows:

$$Q_{\text{new}} = \begin{cases} 0.9 \cdot Q, & \text{if } \|v\| < 1.0 \\ 1.1 \cdot Q, & \text{if } \|v\| > 10.0 \\ Q, & \text{otherwise} \end{cases} \quad (5)$$

The Q_{new} is the noise covariance, Q is the original process noise covariance, $\mathbf{v} = [state_1, state_2]$ represents the first two components of the state vector (assumed to be velocity components), $\|v\| = \sqrt{state_1^2 + state_2^2}$ is the Euclidean norm (L2 norm) of the velocity vector. This formula expresses the following logic: If the norm of the velocity is less than 1.0, Q is reduced by 10%. If the norm of the velocity is greater than 10.0, Q is increased by 10%. If the norm of the velocity is between 1.0 and 10.0, Q remains unchanged.

This dynamic adjustment strategy aims to adjust the Kalman filter's process model based on the current state (in this case, velocity). When the velocity is low, it decreases the process noise (reduces Q), indicating higher confidence in the system dynamics;

when the velocity is high, it increases the process noise (increases Q), indicating lower confidence in the system dynamics.

Autonomous vehicles encounter diverse environmental conditions during operation, such as urban streets, highways, and adverse weather. Dynamic adjustment of R and Q enables the Kalman filter to adapt to these varying conditions, enhancing tracking accuracy by increasing measurement uncertainty in rainy conditions and decreasing it in clear weather. Sensor performance in autonomous vehicles may fluctuate due to factors like temperature, vibration, or partial occlusion. Dynamic R adjustment compensates for these variations. Optimal noise parameters may differ for near and far target tracking, with Q allowing more precise tracking at close range and greater uncertainty at longer distances.

3.5 Life-cycle Adjustment

Threshold adjustment significantly impacts object detection and tracking performance. The **Intersection over Union (IoU)** threshold determines the trade-off between precision and recall. A higher threshold ensures more accurate detections but may miss objects with slightly lower IoU. Conversely, a lower threshold increases sensitivity, potentially detecting more objects at the risk of false positives. Through extensive experimentation, we iteratively optimize this threshold to achieve a balance between detection accuracy and false alarm rate, thereby enhancing the overall system performance in autonomous driving scenarios.

In the life-cycle management stage, compared to the baseline Fast-Poly, Easy-Poly improve in terms of the motion model. We adjusted the wheelbase ratio and rear tire ratio parameters, finding the optimal values through grid search or Bayesian optimization, changing them from the original 0.8 and 0.5 to the latest 0.6 and 0.3. Through these adjustments, tracking performance and robustness have been improved. In addition, we proposed increasing the maximum age parameter to 20 for all detection and tracking categories. This modification significantly extends object tracking duration while maintaining high tracking accuracy and computational efficiency. Consequently, we observed a substantial reduction in frame loss during life-cycle management, resulting in more complete and robust tracking trajectories for each object of interest.

4 EXPERIMENTS

4.1 Datasets

The nuScenes dataset [3] consists of 850 training and 150 test sequences, capturing a wide range of driving scenarios, including challenging weather conditions and nighttime environments. Each sequence contains approximately 40 frames, with keyframes sampled at 2Hz and fully annotated. The official evaluation protocol utilizes **AMOTA**, **MOTA**, and **sAMOTA** [29] as primary metrics, evaluating performance across seven object categories: Car (*Car*), Bicycle (*Bic*), Motorcycle (*Moto*), Pedestrian (*Ped*), Bus (*Bus*), Trailer (*Tra*), and Truck (*Tru*). Notably, Poly-MOT, Fast-Poly, and our proposed Easy-Poly methods exclusively utilize keyframes for tracking tasks.

4.2 Implementation Details

Our tracking framework is implemented in Python and executed on an Nvidia 4090X GPU. Hyperparameters are optimized based on

the highest AMOTA achieved on the validation set. The following category-specific and SF thresholds are employed for nuScenes: (*Bic*: 0.15; *Car*: 0.16; *Moto*: 0.16; *Bus*: 0.12; *Tra*: 0.13; *Tru*: 0; *Ped*: 0.13). NMS thresholds are uniformly set to 0.08 across all categories and datasets. Additionally, we implement Scale-NMS [11] for (*Bic*, *Ped*) categories on nuScenes. In conjunction with the default in NMS, we introduce our novel metric to enhance similarity assessment for (*Bic*, *Ped*, *Bus*, *Tru*) categories on nuScenes. Motion models and filters are consistent with those described in [16]. A lightweight filter, implemented as a median filter with σ , is applied across all datasets. Association metrics universally employ across all datasets. Category-specific first association thresholds for nuScenes are as follows: (*Bic*, *Moto*, *Bus*: 1.6; *Car*, *Tru*: 1.2; *Tra*: 1.16; *Ped*: 1.78). The voxel mask size is set to 5m on nuScenes. Count-based and output file strategies align with those presented in [16]. In the confidence-based component, category-specific decay rates for nuScenes are: (*Ped*: 0.18; *Car*: 0.26; *Tru*, *Moto*: 0.28; *Tra*: 0.22; *Bic*, *Bus*: 0.24). The delete thresholds are set as follows: (*Bus*: 0.08, *Ped*: 0.1, and 0.04 for all other categories) on nuScenes.

In the object tracking phase of 3D MOT, Easy-Poly exhibits exceptional performance following a series of optimizations. These enhancements include pre-processing, Kalman filtering, motion modeling, and tracking cycle refinements. The integration of these techniques significantly improves the algorithm’s effectiveness in complex 3D environments.

Easy-Poly exhibits exceptional performance on the test set, achieving a **75.9%** AMOTA score, surpassing the majority of existing 3D MOT methods. As shown in Table 2, Easy-Poly attains a remarkably low IDS count of **287** while maintaining the highest AMOTA (**75.9%**) among all modal methods. This underscores Easy-Poly’s ability to maintain stable tracking without compromising recall. Notably, Easy-Poly achieves state-of-the-art performance without relying on additional image data input. Easy-Poly significantly outperforms competing algorithms in the critical ‘Car’ category. With minimal computational overhead, it delivers impressive results, highlighting its potential for integration into real-world autonomous driving systems. The False Negative and False Positive metrics in Table 2 further demonstrate Easy-Poly’s robust continuous tracking capability while maintaining high recall.

For validation set experiments in Table 3, we utilize Center-Point [31] as the detector to ensure fair comparisons. As illustrated in Table 3, Easy-Poly significantly outperforms most deep learning-based methods in both tracking accuracy (**75.0%** AMOTA, **64.8%** MOTA) and computational efficiency (**34.9 FPS**). Compared to the baseline FastPoly [15], Easy-Poly achieves substantial improvements of **+1.3%** in MOTA and **+1.6%** in AMOTA, while operating **1.5x** faster under identical conditions. When integrated with the high-performance LargeKernel3D [6] detector, Easy-Poly demonstrates even more impressive detection and tracking capabilities. Furthermore, when employing the multi-camera detector DETR3D [28] with constrained performance, Easy-Poly exhibits robust real-time performance without compromising accuracy. Furthermore, the lower AMOTP and IDS metrics demonstrate Easy-Poly’s exceptional capability in tracking small objects and maintaining performance in complex scenarios and adverse weather conditions. These results underscore the algorithm’s robustness across diverse and challenging environments.

Table 2: A comparison between our proposed method with other advanced methods on the nuScenes test set. ‡ means the GPU device. The reported runtimes of all methods exclude the detection time. Poly-MOT [16], Fast-Poly [15] and Easy-Poly rely entirely on the detector input, as they do not utilize any visual or deep features during tracking.

Method	Device	Detector	Input	AMOTA↑	MOTA↑	FPS↑	IDS↓	FN↓	FP↓
EagerMOT [12]	–	CenterPoint [31]&Cascade R-CNN [4]	2D+3D	67.7	56.8	4	1156	24925	17705
CBMOT [2]	I7-9700	CenterPoint [31]&CenterTrack [34]	2D+3D	67.6	53.9	80.5	709	22828	21604
Minkowski [9]	TITAN‡	Minkowski [9]	3D	69.8	57.8	3.5	325	21200	19340
ByteTrackv2 [33]	–	TransFusion-L [1]	3D	70.1	58	–	488	21836	18682
3DMOTFormer [7]	2080Ti‡	BEVFusion [18]	2D+3D	72.5	60.9	54.7	593	20996	17530
Poly-MOT [16]	9940X	LargeKernel3D [6]	2D+3D	75.4	62.1	3	292	17956	19673
Fast-Poly [15]	7945HX	LargeKernel3D [6]	2D+3D	75.8	62.8	34.2	326	18415	17098
Easy-Poly (Ours)	4090Ti‡	LargeKernel3D [6]	2D+3D	75.9	63.0	34.9	287	17620	16718

Table 3: A comparison of existing methods applied to the nuScenes val set.

Method	Detector	Input Data	MOTA↑	AMOTA↑	AMOTP↓	FPS↑	IDS↓
CBMOT [2]	CenterPoint [31] & CenterTrack [34]	2D + 3D	–	72.0	48.7	–	479
EagerMOT [12]	CenterPoint [31] & Cascade R-CNN [4]	2D + 3D	–	71.2	56.9	13	899
SimpleTrack [22]	CenterPoint [31]	3D	60.2	69.6	54.7	0.5	405
CenterPoint [31]	CenterPoint [31]	3D	–	66.5	56.7	–	562
OGR3MOT [32]	CenterPoint [31]	3D	60.2	69.3	62.7	12.3	262
Poly-MOT [16]	CenterPoint [31]	3D	61.9	73.1	52.1	5.6	281
Poly-MOT [16]	LargeKernel3D-L [6]	3D	54.1	75.2	54.1	8.6	252
Fast-Poly [15]	CenterPoint [31]	3D	63.2	73.7	–	28.9	414
Easy-Poly (Ours)	CenterPoint [31]	2D + 3D	64.4	74.5	54.9	34.6	272
Easy-Poly (Ours)	LargeKernel3D [6]	2D + 3D	64.8	75.0	53.6	34.9	242

Table 4: Comparing different data association algorithms using CenterPoint and (lines 1-7) and LargeKernel3D (lines 8-11) methods on nuScenes val set. Among them, the algorithms lines 1-3 are the Fast-Poly framework and in lines 4-11 are the latest our Easy-Poly framework.

Algorithms	MOTA↑	AMOTA↑	AMOTP↓	IDS↓	FN↓
MNN	62.2	72.5	52.4	433	16644
Greedy	62.3	72.7	53.4	428	17647
Hungarian	63.2	73.7	52.1	414	15996
MNN (Ours)	63.7	73.6	54.8	406	15873
Greedy (Ours)	64.0	73.7	54.6	368	16736
Hungarian (Ours)	64.3	74.3	54.3	335	16892
DTO (Ours)	64.4	74.5	54.9	272	16982
MNN (Ours)	64.1	73.9	54.0	370	15865
Greedy (Ours)	64.5	74.3	53.7	307	16014
Hungarian (Ours)	64.7	74.8	53.9	291	15923
DTO (Ours)	64.8	75.0	53.6	242	15488

4.3 Comparative Evaluations

In this study, we conduct a comprehensive evaluation of the association stage, focusing on four algorithms: Hungarian, Greedy,

MNN, and the novel DTO. Our extensive experiments, summarized in Table 4, reveal that the Easy-Poly consistently outperforms Fast-Poly across both CenterPoint and LargeKernel3D frameworks. Notably, LargeKernel3D demonstrates superior performance over CenterPoint, particularly in complex tracking scenarios. Among the association algorithms, Hungarian and DTO consistently yield superior results, underscoring their robustness and efficacy in diverse multi-object tracking contexts. Compared to the Hungarian algorithm, DTO not only achieves similarly excellent AMOTA values but also provides more robust and accurate tracking performance, especially in challenging scenarios involving occlusions, missed detections, or false positives. These findings highlight the critical role of algorithm selection and model optimization in advancing the state-of-the-art in 3D object tracking.

Table 5 demonstrates the efficacy of our proposed methods. The Fast-Poly tracklet termination strategy (line 3) significantly outperforms baseline score refinement [2] (line 2), yielding a **2.7%** improvement in AMOTA and reducing FN by **2366**. This enhancement mitigates tracker vulnerabilities in mismatch scenarios, including occlusions. Further performance gains are achieved through smoother score prediction (line 4), resulting in additional improvements of **0.4%** AMOTA, **0.1%** MOTA, and a reduction of **926 FN**. Our Easy-Poly model exhibits even more substantial performance enhancements. The tracklet termination strategy (line 7) surpasses the baseline score refinement (line 6) by **2.8%** in AMOTA while

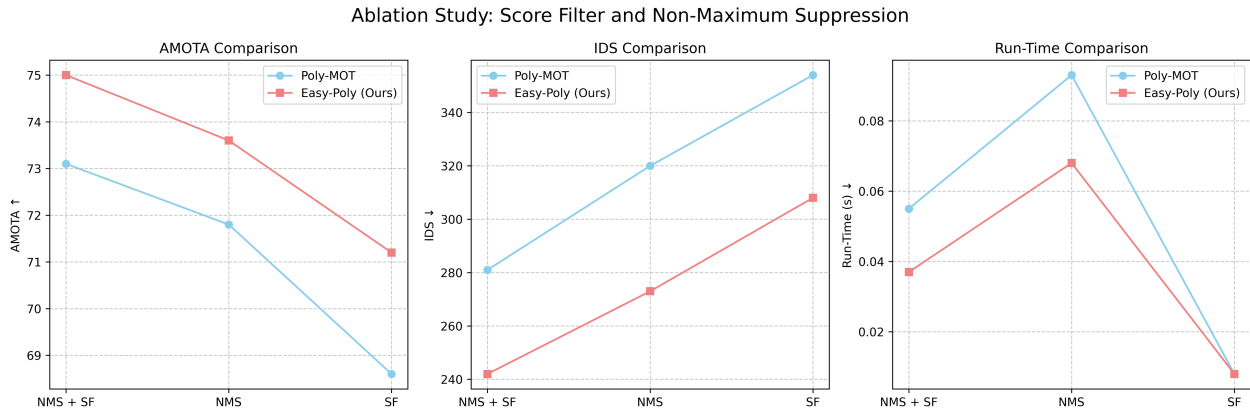


Figure 3: The ablation study of whether or not to use Score Filter and Non-Maximum Suppression, including the Run-Time, which represents the execution time of the Pre-processing Module. We compared Poly-MOT with our proposed Easy-Poly method.

Table 5: A comparison on distinct life-cycle modules on nuScenes val set. Average means using the online average score to delete. Latest means using the latest score to delete. Max-age means using the continuous mismatch time to delete. Other settings are under the best performance. Methods in lines 1-4 and lines 5-8 use Fast-Poly [15] and Our Easy-Poly.

Strategy	AMOTA↑	MOTA↑	FPS↑	FN↓
Count & Max-age	73.3	62.9	23.0	16523
Confidence [2] & Latest	70.6	63.2	45.8	19192
Confidence [2] & Average	73.3	63.1	28.3	16826
Confidence & Average	73.7	63.2	28.9	15900
Count & Max-age (Ours)	74.3	63.8	34.3	16024
Confidence [2] & Latest (Ours)	71.8	63.7	50.2	17907
Confidence [2] & Average (Ours)	74.6	64.2	35.6	16063
Confidence & Average (Ours)	75.0	64.8	36.9	15488

decreasing FN by **1844**. Furthermore, the integration of smoother score prediction (line 8) further boosts the tracking performance, resulting in improvements of **0.4%** in AMOTA and **0.6%** in MOTA, along with a reduction of **575 FN**.

4.4 Ablation Studies

We optimize two-stage filtering approach that synergistically combines SF and NMS to significantly enhance bounding box quality in multi-object tracking scenarios. This novel method effectively integrates SF to eliminate low-score detections and NMS to remove high-confidence duplicates, resulting in a set of superior quality bounding boxes. Our comprehensive experimental results, presented in Figure 3, demonstrate substantial improvements in both computational efficiency and tracking accuracy across multiple state-of-the-art models. For the Poly-MOT model, our approach of applying SF before NMS yields a remarkable **40%** reduction in pre-processing inference time while simultaneously improving AMOTA

by **1.3%** compared to using NMS alone. These results highlight the significant potential of our method in improving real-time tracking capabilities without compromising accuracy. The Easy-Poly model exhibits even more impressive performance gains, further validating the scalability and effectiveness of our approach. By applying SF before NMS, we achieve a substantial **50%** reduction in pre-processing time coupled with a **1.4%** improvement in AMOTA. This notable improve in both speed and accuracy underscores the robustness of our method across different model architectures. Importantly, our analysis reveals critical insight into the interplay between SF and NMS. Although using SF without NMS accelerates processing, it leads to significant degradation in both AMOTA and Identity Switches IDS metrics. This observation underscores the crucial importance of our combined SF-NMS approach in maintaining an optimal balance between processing speed and tracking accuracy. The synergistic effect of SF and NMS not only enhances the quality of bounding boxes but also optimizes the trade-off between computational efficiency and tracking performance. This balance is particularly vital in real-world applications where both speed and accuracy are paramount, such as autonomous driving and surveillance systems.

5 CONCLUSION

In this paper, we presented Easy-Poly, a real-time 3D multi-object tracking system that integrates refined detection and robust tracking within a unified pipeline. By employing an augmented proposal generator with improved sparse convolutions and multi-modal data augmentation, we significantly enhanced detection accuracy and speed, especially in dense traffic and small-object scenarios. Our framework also incorporates score filtering, non-maximum suppression, a dynamic track-oriented association module, and a dynamic motion modeling strategy with adaptive Kalman filtering and confidence weighting. Experiments on the nuScenes dataset show that Easy-Poly outperforms existing baselines in both detection and tracking metrics, demonstrating stronger robustness in challenging and adverse conditions.

REFERENCES

- [1] Xuyang Bai, Zeyu Hu, Xinge Zhu, Qingqiu Huang, Yilun Chen, Hongbo Fu, and Chiew-Lan Tai. 2022. Transfusion: Robust lidar-camera fusion for 3d object detection with transformers. In *CVPR*. 1090–1099.
- [2] Nuri Benbarka, Jona Schröder, and Andreas Zell. 2021. Score refinement for confidence-based 3D multi-object tracking. In *IROS*. IEEE, 8083–8090.
- [3] Holger Caesar, Varun Bankiti, Alex H Lang, Sourabh Vora, Venice Erin Liong, Qiang Xu, Anush Krishnan, Yu Pan, Giancarlo Baldan, and Oscar Beijbom. 2020. nuscenes: A multimodal dataset for autonomous driving. In *Proceedings of the IEEE/CVF conference on computer vision and pattern recognition*. 11621–11631.
- [4] Zhaowei Cai and Nuno Vasconcelos. 2018. Cascade r-cnn: Delving into high quality object detection. In *CVPR*. 6154–6162.
- [5] Yukang Chen, Yanwei Li, Xiangyu Zhang, Jian Sun, and Jiaya Jia. 2022. Focal sparse convolutional networks for 3d object detection. In *CVPR*. 5428–5437.
- [6] Yukang Chen, Jianhui Liu, Xiaojuan Qi, Xiangyu Zhang, Jian Sun, and Jiaya Jia. 2022. Scaling up kernels in 3d cnns. *arXiv preprint arXiv:2206.10555* (2022).
- [7] Shuxiao Ding, Eike Rehder, Lukas Schneider, Marius Cordts, and Juergen Gall. 2023. 3dmtformer: Graph transformer for online 3d multi-object tracking. In *ICCV*. 9784–9794.
- [8] Runzhou Ge, Zhuangzhuang Ding, Yihan Hu, Yu Wang, Sijia Chen, Li Huang, and Yuan Li. 2020. Afdet: Anchor free one stage 3d object detection. *arXiv preprint arXiv:2006.12671* (2020).
- [9] JunYoung Gwak, Silvio Savarese, and Jeannette Bohg. 2022. Minkowski tracker: A sparse spatio-temporal R-CNN for joint object detection and tracking. *arXiv preprint arXiv:2208.10056* (2022).
- [10] Martin Hahner, Dengxin Dai, Alexander Liniger, and Luc Van Gool. 2020. Quantifying data augmentation for lidar based 3d object detection. *arXiv preprint arXiv:2004.01643* (2020).
- [11] Junjie Huang, Guan Huang, Zheng Zhu, Yun Ye, and Dalong Du. 2021. Bevdet: High-performance multi-camera 3d object detection in bird-eye-view. *arXiv preprint arXiv:2112.11790* (2021).
- [12] Aleksandr Kim, Aljoša Ošep, and Laura Leal-Taixé. 2021. Eagermot: 3d multi-object tracking via sensor fusion. In *ICRA*. IEEE, 11315–11321.
- [13] Harold W Kuhn. 1955. The Hungarian method for the assignment problem. *Naval research logistics quarterly* 2, 1-2 (1955), 83–97.
- [14] Alex H Lang, Sourabh Vora, Holger Caesar, Lubing Zhou, Jiong Yang, and Oscar Beijbom. 2019. Pointpillars: Fast encoders for object detection from point clouds. In *Proceedings of the IEEE/CVF conference on computer vision and pattern recognition*. 12697–12705.
- [15] Xiaoyu Li, Dedong Liu, Yitao Wu, Xian Wu, Lijun Zhao, and Jinghan Gao. 2024. Fast-poly: A fast polyhedral framework for 3d multi-object tracking. *arXiv preprint arXiv:2403.13443* (2024).
- [16] Xiaoyu Li, Tao Xie, Dedong Liu, Jinghan Gao, Kun Dai, Zhiqiang Jiang, Lijun Zhao, and Ke Wang. 2023. Poly-mot: A polyhedral framework for 3d multi-object tracking. In *2023 IEEE/RSJ International Conference on Intelligent Robots and Systems (IROS)*. IEEE, 9391–9398.
- [17] Yen-Cheng Liu, Chih-Yao Ma, and Zsolt Kira. 2022. Unbiased teacher v2: Semi-supervised object detection for anchor-free and anchor-based detectors. In *CVPR*. 9819–9828.
- [18] Zhijian Liu, Haotian Tang, Alexander Amini, Xinyu Yang, Huizi Mao, Daniela L Rus, and Song Han. 2023. Bevfusion: Multi-task multi-sensor fusion with unified bird’s-eye view representation. In *ICRA*. IEEE, 2774–2781.
- [19] Su Pang, Daniel Morris, and Hayder Radha. 2020. CLOCs: Camera-LiDAR object candidates fusion for 3D object detection. In *IROS*. IEEE, 10386–10393.
- [20] Su Pang, Daniel Morris, and Hayder Radha. 2022. Fast-CLOCs: Fast camera-LiDAR object candidates fusion for 3D object detection. In *Proceedings of the IEEE/CVF Winter Conference on Applications of Computer Vision*. 187–196.
- [21] Ziqi Pang, Jie Li, Pavel Tokmakov, Dian Chen, Sergey Zagoruyko, and Yu-Xiong Wang. 2023. Standing Between Past and Future: Spatio-Temporal Modeling for Multi-Camera 3D Multi-Object Tracking. In *CVPR*. 17928–17938.
- [22] Ziqi Pang, Zhichao Li, and Naiyan Wang. 2022. Simpletrack: Understanding and rethinking 3d multi-object tracking. In *ECCVW*. Springer, 680–696.
- [23] Charles R Qi, Wei Liu, Chenxia Wu, Hao Su, and Leonidas J Guibas. 2018. Frustum pointnets for 3d object detection from rgb-d data. In *CVPR*. 918–927.
- [24] Rui Qian, Xin Lai, and Xirong Li. 2022. 3d object detection for autonomous driving: a survey. *Pattern Recognition* 130 (2022), 108796.
- [25] Tara Sadjadpour, Jie Li, Rares Ambrus, and Jeannette Bohg. 2023. Shasta: Modeling shape and spatio-temporal affinities for 3d multi-object tracking. *RA-L* (2023).
- [26] Li Wang, Xinyu Zhang, Wenyan Qin, Xiaoyu Li, Jinghan Gao, Lei Yang, Zhiwei Li, Jun Li, Lei Zhu, Hong Wang, et al. 2023. Camo-mot: Combined appearance-motion optimization for 3d multi-object tracking with camera-lidar fusion. *T-ITS* (2023).
- [27] Xiyang Wang, Chunyun Fu, Zhankun Li, Ying Lai, and Jiawei He. 2022. DeepFusionMOT: A 3D multi-object tracking framework based on camera-LiDAR fusion with deep association. *RA-L* 7, 3 (2022), 8260–8267.
- [28] Yue Wang, Vitor Campagnolo Guizilini, Tianyuan Zhang, Yilun Wang, Hang Zhao, and Justin Solomon. 2022. Detr3d: 3d object detection from multi-view images via 3d-to-2d queries. In *CoRL*. PMLR, 180–191.
- [29] Xinhua Weng, Jianren Wang, David Held, and Kris Kitani. 2020. 3d multi-object tracking: A baseline and new evaluation metrics. In *IROS*. IEEE, 10359–10366.
- [30] Hai Wu, Wenkai Han, Chenglu Wen, Xin Li, and Cheng Wang. 2021. 3D multi-object tracking in point clouds based on prediction confidence-guided data association. *T-ITS* 23, 6 (2021), 5668–5677.
- [31] Tianwei Yin, Xingyi Zhou, and Philipp Krahenbuhl. 2021. Center-based 3d object detection and tracking. In *CVPR*. 11784–11793.
- [32] Jan-Nico Zaech, Alexander Liniger, Dengxin Dai, Martin Danelljan, and Luc Van Gool. 2022. Learnable online graph representations for 3D multi-object tracking. *RA-L* 7, 2 (2022), 5103–5110.
- [33] Yifu Zhang, Xinggang Wang, Xiaoqing Ye, Wei Zhang, Jincheng Lu, Xiao Tan, Errui Ding, Peize Sun, and Jingdong Wang. 2023. ByteTrackV2: 2D and 3D Multi-Object Tracking by Associating Every Detection Box. *arXiv:2303.15334* [cs.CV]
- [34] Xingyi Zhou, Vladlen Koltun, and Philipp Krähenbühl. 2020. Tracking objects as points. In *ECCV*. Springer, 474–490.